

# Lawrence Berkeley National Laboratory

## Recent Work

### **Title**

On magnetic fluid emplacement: Laboratory Experiments of Ferrofluid Flow

### **Permalink**

<https://escholarship.org/uc/item/7hb4t8t9>

### **Author**

Borglin, Sharon

### **Publication Date**

1998-08-01



# ERNEST ORLANDO LAWRENCE BERKELEY NATIONAL LABORATORY

## On Magnetic Fluid Emplacement: Laboratory Experiments of Ferrofluid Flow

Sharon E. Borglin, George J. Moridis,  
and Curtis M. Oldenburg

**Earth Sciences Division**

August 1998

Submitted to  
*Water Resources Research*



REFERENCE COPY |  
Does Not |  
Circulate |  
Bldg. 50 Library - Ref.  
Lawrence Berkeley National Laboratory

LBNL-42203

## **DISCLAIMER**

This document was prepared as an account of work sponsored by the United States Government. While this document is believed to contain correct information, neither the United States Government nor any agency thereof, nor the Regents of the University of California, nor any of their employees, makes any warranty, express or implied, or assumes any legal responsibility for the accuracy, completeness, or usefulness of any information, apparatus, product, or process disclosed, or represents that its use would not infringe privately owned rights. Reference herein to any specific commercial product, process, or service by its trade name, trademark, manufacturer, or otherwise, does not necessarily constitute or imply its endorsement, recommendation, or favoring by the United States Government or any agency thereof; or the Regents of the University of California. The views and opinions of authors expressed herein do not necessarily state or reflect those of the United States Government or any agency thereof or the Regents of the University of California.

**LBNL 42203**

**On Magnetic Fluid Emplacement:  
Laboratory Experiments of Ferrofluid Flow**

Sharon E. Borglin, George J. Moridis, and Curtis M. Oldenburg

*Earth Sciences Division  
Lawrence Berkeley National Laboratory  
University of California  
Berkeley, California 94720*

*August 1998*

This work was supported by the Laboratory Directed Research and Development Program of Lawrence Berkeley National Laboratory under the U.S. Department of Energy, contract No. DE-AC03-76SF00098

## **Abstract**

This paper presents experimental results of the flow of ferrofluids in porous media to investigate the potential for precisely controlling fluid emplacement using magnetic fields. Ferrofluids are colloidal suspensions of magnetic particles stabilized in various carrier liquids. . In the presence of an external magnetic field, the ferrofluid becomes magnetized as the particles align with the magnetic field. In the presence of a gradient in the magnetic field strength, a magnetic body force is produced on the ferrofluid. The pressures measured in the ferrofluid in the presence of a magnetic field agree well with calculated values. In vertical Hele-Shaw cell and porous media experiments, where vertical gravitational forces and lateral magnetic forces act simultaneously, the magnetic field produces strong holding forces on the ferrofluid near the magnet. The flow experiments demonstrate that the ferrofluid assumes a consistent arc-shaped configuration around the magnet regardless of initial configuration or flow path toward the magnet. The experiments reported here support the concept of using ferrofluids to aid in the precise placement of fluids in porous media in either laboratory or subsurface applications.

## Nomenclature

$B$	magnetic induction, $T$
$B_r$	residual magnetic induction of permanent magnet, $T$
$H$	external magnetic field, $A/m$
$H_x$	x component of the magnetic field, $A/m$
$M$	magnetization, $A/m$
$\bar{M}$	field-averaged magnetization, $A/m$
$M_n$	magnetization normal to the surface, $A/m$
$\mu$	dynamic viscosity, $Pa \cdot s$
$\mu_m$	magnetic permeability, $Tm/A$
$\mu_{mo}$	magnetic permeability of free space, $Tm/A$
$F$	Force, $N$
$p_o$	ambient atmospheric pressure, $Pa$
$p_n$	normal pressure, $Pa$
$p_c$	capillary pressure, $Pa$
$p_G$	magnetopressure (gage), $Pa$
$\rho$	density, $kg/m^3$
$g$	gravitational acceleration, $m/s^2$
$2a$	height of permanent magnet, $m$
$2b$	width of permanent magnet, $m$
$L_o$	length of permanent magnet, $m$
$x$	distance along centerline of magnetic pole, $m$
$y$	distance perpendicular to magnetic pole, $m$
$z$	distance perpendicular to magnetic pole, $m$
$K$	hydraulic conductivity, $m/s$
$k$	permeability of porous media, $m^2$
$a$	gap width of Hele-Shaw cell, $m$

## 1. Introduction

Ferrofluids are stable colloidal suspensions of magnetic particles in various carrier liquids [Raj and Moskowitz, 1990]. The solid, magnetic, single-domain particles are small (with an average diameter of 10 nm) and are covered with a molecular layer of a dispersant. In the presence of an external magnetic field, the ferrofluid becomes magnetized as the particles align with the magnetic field. In the presence of a gradient in the magnetic field strength, a magnetic body force is produced on the ferrofluid. Thermal agitation due to Brownian motion keeps the particles suspended, while the dispersant coating inhibits agglomeration. A ferrofluid is stable, as neither an external magnetic field nor gravity can separate the magnetic particles from the carrier liquid. Consequently, pure ferrofluids behave like a homogeneous single-phase fluid that can be magnetized when placed in a strong magnetic field. Because of the small size of the ferromagnetic particles, ferrofluids can flow through porous media such as natural sediments or fractured rock due to gravitational, pressure gradient, capillary, and magnetic forces. The attractive magnetic forces generated between a permanent magnet and a ferrofluid allows the ferrofluid to be manipulated to flow in any desired direction through control of the external magnetic field and without any direct physical contact [Chorney and Mraz, 1992].

The potential of controlling fluid motion in porous media, without direct access to the fluid, is compelling. Potentially significant applications include controlled emplacement of subsurface barrier liquids or treatment chemicals, as well as emplacement of geophysically imaggable liquids into particular zones for subsequent imaging [Moridis *et al.*, 1998]. In this paper, we present a series of experiments aimed at demonstrating the forces and flows that can be

produced in a ferrofluid or ferrofluid-water mixtures due to external magnetic fields produced by permanent magnets. The experiments demonstrate the ability of permanent magnets to mobilize ferrofluid and to control the final configuration of injected ferrofluid. While our ultimate objective is the development of novel subsurface environmental remediation solutions, our results to date have been limited to laboratory length scales up to approximately 0.25 m. As such, our results are particularly relevant to laboratory work where ferrofluids may find immediate application in any situation where it is desirable to control the motion or final configuration of fluid in an experimental flow apparatus. Extension of results presented here to larger length scales and field-scale applications must await further study.

## 2. Magnetic Properties of Ferrofluids

### 2.1 Ferrofluid Magnetization

The study of ferrofluids involves traditional ferromagnetic principles. In the absence of a magnetic field, ferrofluid particles are randomly oriented, the fluid has no net magnetization, and there is no long-range order between the colloidal ferrofluid particles. In the presence of an external magnetic field, ferrofluid particles align with the field and the ferrofluid becomes magnetized. The relationship between the induced field,  $B$ , the external magnetic field,  $H$ , and the intensity of magnetization,  $M$ , of a ferrofluid is given by

$$B = \mu_m (H + M) \quad (1)$$

where  $\mu_m$  is the magnetic permeability of the medium. For free space (i.e., air),  $\mu_m = \mu_{m0}$ , which has the value of  $4\pi \times 10^{-7}$  Tm/A (Tesla-meter/Ampere). In soft magnetic materials such as



ferrofluid,  $M$  and  $H$  are aligned which allows us to equate the vector quantities  $M$  and  $H$  with the magnitudes  $M$  and  $H$  in relations such as Equation 1. Equation 1 shows that magnetic induction has contributions from the external field and from magnetization. Figure 1 illustrates the magnetization curve [Nunes and Yu, 1987] for a commercially available ferrofluid, EMG 805<sup>TM</sup>, (Ferrofluidics Corp., Nashua, NH). The total magnetic induction (Equation 1) would be formed by adding the magnetization ( $M$ ), plotted in Figure 1, with the external magnetic field ( $H$ ) and multiplying by the magnetic permeability ( $\mu_m$ ).

Figure 1 also shows that, ferrofluids behave as soft magnetic materials with a saturation magnetization. That is, small changes in the external magnetic field result in substantial magnetization changes as long as external magnetic field strength is weaker than the value at which the ferrofluid reaches saturation. For the ferrofluid plotted in Figure 1, the saturation magnetization is approximately  $1.6 \times 10^4$  A/m, which is reached when the external magnetic field strength is larger than approximately  $6 \times 10^5$  A/m.

## 2.2 Ferrofluid Force

Equations for ferrofluid flow have been presented by Rosensweig [1985]. For our purposes, it will suffice to show only the fundamental force equation relating the body force on a ferrofluid to the magnetization and gradient of the external magnetic field. This body force, when manifested in a fluid, has been referred to as “magnetopressure” by Moridis and Oldenburg [1998], and is given by

$$F = \mu_m M \nabla H . \quad (2)$$

This simple equation controls many of the fundamental aspects of ferrofluid flow. In particular, note that since  $M$  and  $H$  are aligned, ferrofluids are always attracted toward magnets regardless of the orientation of the magnet. Furthermore, the force is proportional to the magnetization, which as shown in Figure 1, is a strong function of the external magnetic field strength ( $H$ ) when  $H$  is small, but is constant once the ferrofluid has reached saturation. Finally, the force on ferrofluid is also proportional to the gradient of the external magnetic field. The combination of these effects produces very strong forces on ferrofluid when the ferrofluid is near a permanent magnet, because the ferrofluid is at or near saturation and the gradient of the external magnetic field is very steep. Conversely, Equation 2 shows that the force on ferrofluid becomes very small when the magnet and the ferrofluid are separated by a significant distance, e.g. more than approximately 0.5 m for typical ferrofluid-magnet combinations used in the current study. The generation of strong ferrofluid attraction when the fluid is near the magnet and weak forces at distance from the magnet are demonstrated in the experiments presented below.

### 3. Materials

#### 3.1 Ferrofluid

In this study we used two ferrofluids, EMG 805<sup>TM</sup> (FF1) and EMG-C<sup>TM</sup> (FF2) (Ferrofluids Corporation, Nashua, NH). Table 1 summarizes the physical properties of the two fluids. Both of these ferrofluids are aqueous ferrofluids, because they use water as the carrier liquid. The larger magnetite concentration in FF2 gives this fluid a higher saturation

magnetization. The stabilization of the magnetic particles is achieved by means of a water-soluble dispersant (surfactant). To avoid potential interaction between the negatively-charged soil particles and the ferrofluid, both ferrofluids were selected with anionic dispersants at neutral pH. All the concentrations given in Table 1 are by volume.

### 3.2 Porous Media

The porous media used in the experiments are described in Table 2. Monterey #60 sand (RMC Lonestar, Pleasanton, CA), and Unimin 30/40 mesh silica sand (Unimin Corp., Le Sueur, MN), hereafter referred to as S1 and S2, are commercially available.

### 3.3 Permanent Magnets

Neodymium iron boron (NdFeB) permanent magnets were used to create the magnetic fields in the experiments (Table 3). For ease of differentiation, the magnets are referred to as PM1 (Pacimax 35H, Pacific Century Enterprises, Centreville, VA) and PM2 (courtesy of R. Schlueter, Advanced Light Source, LBNL). As shown in Figure 2, the terms  $2a$  and  $2b$  refer to the height and width of the rectangular permanent magnets. Five units of the PM1 magnets were often used in a stacked arrangement, which was equivalent to a single magnet with length ( $L_o$ ) = 0.127 m.

The 3-dimensional magnetic fields created by a rectangular permanent magnet (such as the NdFeB blocks) can be described by the analytical expressions of McCaig and Clegg, [1987]. The equation for the  $x$  component of the magnetic field simplifies to

$$H_x = \frac{B_r}{\pi\mu_m} \left[ \tan^{-1} \left( \frac{ab}{x(a^2 + b^2 + x^2)^{\frac{1}{2}}} \right) - \tan^{-1} \left( \frac{ab}{(x + L_o)(a^2 + b^2 + (x + L_o)^2)^{\frac{1}{2}}} \right) \right] \quad (3)$$

where  $x$  is the position along the centerline of the magnet (see Figure 2).  $B_r$ , the residual induction of the permanent magnets, represents the maximum flux output from the given magnet.

Equation 3 was verified for the PM1 and PM2 magnets by measuring the magnetic field using a DTM 141-G Group 3 Teslameter equipped with a LPT-141 probe (Group 3 Technology Ltd., Auckland, NZ). Figure 3 shows excellent agreement between measurements and analytical predictions of the field created by five stacked PM1 magnets.

## 4. Experimental Studies

### 4.1 Introduction

The experiments discussed in this section were designed to demonstrate the generation of magnetic forces on ferrofluid, the mobilization of ferrofluid in response to an external magnetic field created by a permanent magnet, and the static hold that permanent magnets can exert on ferrofluids. The experiments presented include demonstrations and measurements of (1) magnetopressure, (2) magnetically induced flow through horizontal and vertical porous media analog cells, and (3) magnetically induced ferrofluid flow through porous media.

### 4.2 Magnetopressure

In this experiment, we placed ferrofluid in a magnetic field and measured the pressure induced by the magnetic attraction of ferrofluid toward the magnet. The apparatus consisted of a

horizontal column filled with ferrofluid connected at one end to a differential pressure transducer (DPT), with the other end open to the atmosphere (Figure 4). The ferrofluid column in this experiment had a length of 12 cm, with an inside diameter of 0.95 cm. To avoid magnetic effects on its metallic and electronic components, the DPT was connected to the column by means of a flexible nylon tube filled with Dow Corning 200 fluid silicone oil (Dow Corning Corporation, Midland, MI), which served as a pressure-transfer liquid. The silicone-filled tube was 1.3 m long and had an inner diameter of 0.18 cm. To cover the range of the magnetopressures measured in this experiment, three different transducers were used: Validyne DPT models DP 15-30, DP 15-26, and DP 15-20 (Validyne Systems, Northridge, CA). The transducers were calibrated with known hydrostatic pressures in a vertical water column. The DPT measurements were recorded electronically using a computer with a Validyne signal conditioning unit operated by a GPIB interface with a LabView™ (National Instruments, Austin, TX) data acquisition program.

Pressure measurements were recorded as the permanent magnet was placed successively closer to the end of the column connected to the pressure transducer. The 5 stacked PM1 magnets and the PM2 magnet (Table 3) were used in this experiment. The center of the ferrofluid column was aligned with the axis of the magnetic pole. Figures 5 and 6 show the measured magnetopressures,  $p_G$  (gage pressures), in horizontal columns filled with the FF1 and FF2 fluids, respectively.

The magnitude of the magnetopressure ( $p_G$ ) and the distance over which it is effectively exerted increase with the strength and gradient of the magnetic field and the saturation magnetization of the fluid. The dependence of  $p_G$  on the magnetic field can be seen in Figure 5,

which shows the  $p_G$  exerted by the FF2 fluid due to the 5 stacked PM1 magnets and the PM2 magnet. Figure 5 shows a rapid decline in pressure as the magnetic field strength decreases with increasing distance from the pole. The pressures created by the 5 PM1 magnets are larger because of the stronger field strength, due to a higher  $B_r$  value and a longer magnet length (see Equation 3 and Table 3).

The increase in the  $p_G$  with an increase in the fluid magnetization is shown in Figure 6, where the  $p_G$  created by the 5 stacked PM1 magnets in the FF2 fluid is higher than the one created in the FF1 fluid. Although the magnetite particles are identical in the two liquids, the larger concentration of magnetite in the FF2 creates a greater force in the fluid. The close-range measurements in Figures 5 and 6 (i.e., the ones in the immediate vicinity of the pole) include a certain level of uncertainty because the high field strength near the surface of the magnet causes the ferrofluid to spike or separate from the bulk of the fluid in the tube along the ferrofluid-silicone oil interface [Rosensweig, 1985], which in turn affects the pressure measured by the transducer.

The measured magnetopressures can be compared to predicted values, utilizing the magnetization curve of FF1 and the measured field strength of the permanent magnets. Neglecting capillary pressures, the pressure produced in the ferrofluid can be calculated using the ferrohydrodynamic Bernoulli equation [p 178, Rosensweig, 1985] in the following form

$$\Delta p = \mu_{m0} \overline{MH}. \quad (4)$$

Equation 4 was used along with the magnetization curve (Figure 1) and the measured magnetic field data to calculate the magnetopressure. The results are shown in Figures 5 and 6 along with

the measured data. The fit between measurements and predictions is generally good. Some deviation can be expected due to the difficulty of placing the tube directly in the centerline of the large magnet and also due to the above-mentioned formation of spikes at the ferrofluid-silicone oil interface at high magnetic field strength.

### 4.3 Flow in Horizontal Hele-Shaw Cells

The use of Hele-Shaw cells, i.e., parallel glass plates separated by a narrow gap, as experimental analogs of porous media is well documented. The permeability,  $k$ , of a Hele-Shaw cell is given as [Lamb, 1945; Saffman and Taylor, 1958]

$$k = \frac{a^2}{12} \quad (5)$$

where  $a$  is the gap width.

In the following experiments, ferrofluid was injected into water-filled, horizontal Hele-Shaw cells and the ferrofluid movement under the influence of a magnetic field was observed. A significant advantage of Hele-Shaw cells over two-dimensional porous media systems is the ability to visualize the flow. It should be noted, however, that caution must be exercised in the use of Hele-Shaw cells as analogs of porous media. Specifically, equation 5 may not be entirely applicable due to differing wettability characteristics of ferrofluids, because the stabilizing surfactants causes the ferrofluid to have a lower surface tension than pure water. Moreover, if the cell gap is filled with a liquid (such as water) with a density significantly lower than the ferrofluid, gravitational separation may occur. Finally, because the miscibility of a water-based ferrofluid is inhibited by the presence of a magnetic field [Borglin *et al.*, 1998], the liquid between

the cell plates cannot be considered homogeneous, but behaves as a quasi two-phase system, in which solubility is controlled by the magnetic field.

A schematic diagram of the Hele-Shaw cell used in the experiments is shown in Figure 7. The Hele-Shaw cell was constructed from two 0.25 m x 0.28 m glass plates (plate thickness = 6.4 mm). A 1.6 mm shim was placed around the edge and between the plates, the edges of the plates were caulked with silicone, and the cell gap was filled with water. From the volume of water needed to fill the cell, we concluded that the average gap width was 2 mm, which was due to expansion of the cell gap by the emplaced water and the non-planar glass. Using equation 5, this gap width will produce an estimated  $k$  in the Hele-Shaw cell of  $3 \times 10^{-7} \text{ m}^2$ .

The plates were leveled, placed horizontally and 0.3 ml of FF1 ferrofluid was injected using a 20-gauge syringe needle (see Figure 7). Following injection, the syringe was removed and an external magnetic field was applied using the 5 stacked PM1 magnets. The cell gap was centered on the pole face of the magnet, aligned with  $y$ - $z$  plane of the pole face at  $x = 0$  (see Figure 2).

The magnetic field gradient attracted the ferrofluid toward the magnet and the movement was recorded utilizing a time-indexed CCD video camera. A series of images captured from the video of Experiment is shown in Figure 8. Plate (a) shows the initial ferrofluid shape before the application of the external magnetic field. At 219 s, the fluid has moved to form the teardrop shape shown in Plate (b). As the teardrop elongates, the ferrofluid closest to the magnet accelerates, because it encounters a higher magnetic field strength and a steeper field gradient. In Plate (c) at 277 s, the fluid acceleration is sufficiently large to result in small-scale turbulence,



which appear as fingers in the advancing ferrofluid front. In Plate (d) at 427 s, the fluid has reached the sealed end of the Hele-Shaw cell and is accumulating symmetrically around the magnet. The fluid continues migrating until the bulk of the fluid accumulates against the magnet forming a symmetric, arc-shaped pool.

Despite the nominal water miscibility of FF1, mixing with the water in the cell gap is very limited in this experiment. When mixing occurs, it is indicated by a lighter-gray halo around the ferrofluid. A determination of ferrofluid dilution by direct observation is difficult due to the opacity of the ferrofluid-water mixture even at low concentrations. In the magnetic segregation experiments described in Borglin *et al.* [1998], it was determined that even diluted ferrofluid, on the order of 1%, was visually indistinguishable from the pure ferrofluid. These segregation experiments, however, demonstrated that any mixing, especially in the presence of a magnetic field, is limited and reversible. This is attributed to the strong attractive forces between the ferrofluid and the magnet, and the resulting magnetically-controlled miscibility.

The flow of ferrofluid in the Hele-Shaw cell in this experiment was slower than that predicted from the estimated  $k$  of  $3 \times 10^{-7} \text{ m}^2$  calculated from Equation 5 for an average gap width of 2 mm. The higher density and viscosity of FF1 could have accounted for the slower rate, although some of these effects could have been counter-balanced by the lower surface tension of the ferrofluid. Specifically, from the size of the disk formed in the initial injection of the ferrofluid into the Hele-Shaw cell and the known volume of fluid injection, the initial thickness of the ferrofluid in the experiment (Figure 8, Plate a) was estimated to be 0.067 mm, or 1/30th of the gap width. This indicated that the fluid had spread in a thin layer on the bottom of the gap due

its the higher (specific gravity 1.2). The estimated permeability experienced by the ferrofluid based on this effective gap width is calculated to be  $4 \times 10^{-8} \text{ m}^2$  using equation 5. However, in this experiment the FF1 fluid only contacts the lower plate while the top surface interacts with the water in the cell gap causing the requirements of the Hele-Shaw analogy to be unfulfilled in this case. Other experiments using roughened glass plates and neutral density background fluids were carried out and showed good agreement with numerical simulation [Oldenburg *et al.*, 1998].

We observed throughout our experiments with Hele-Shaw cells the significant feature that regardless of the initial ferrofluid configuration or pathway to the magnet, ferrofluid accumulates invariably in a symmetric, arc-shaped pool around the magnet. This predictable and reproducible shape has potentially important implications for subsurface environmental applications in the field and the laboratory. For example, a series of injections followed by periods of magnetic attraction could be used to accumulate a ferrofluid mixed with a reactant or barrier liquid against a magnet, thus covering the target zone by a series of overlapping fluid spheres.

#### **4.4 Flow in a Vertical Hele-Shaw Cell**

To investigate the simultaneous interaction of gravity and magnetic force in ferrofluid flow, a smooth-glass Hele-Shaw cell with a gap width of 1 mm and dimensions of 0.25 m x 0.25 m was oriented vertically and filled with water (see Figure 9). Three sides of the cell were sealed with silicone, and the top edge was left open to the atmosphere. The 5 stacked PM1 magnets were placed alongside the cell, 0.15 m from the cell bottom, with the pole of the magnet oriented with the center of the gap.

FF2 ferrofluid with specific gravity of 1.2 was injected into the water at three different locations in the cell 0.01 m below the cell top. Gravity and magnetic attraction act to pull the ferrofluid downward and to the side, respectively. At a distance of 17 cm from the magnet, magnetic attraction was larger than the gravitational force and all of the ferrofluid accumulated next to the magnet. At a distance of 20 cm the competition between gravity and magnetic attraction is more balanced: the majority of the fluid accumulated near the magnet, with a portion falling under gravity to the bottom of the cell as the magnetic field did not have sufficient time to act on it. At a distance of 22 cm, the magnetic field is weak: all of the injected ferrofluid fell to the bottom of the cell. Over time, the ferrofluid attracted to the magnet formed a static arc-shaped pool around the magnet. The shape of the accumulation of the ferrofluid around the magnet is similar to that observed in the horizontal cells. This experiment demonstrates the strong magnetic attraction of ferrofluid toward the magnet when the ferrofluid is less than about 20 m from the magnet, and the relative strength of gravity when the ferrofluid is farther from the magnet. We emphasize that in both the horizontal and vertical Hele-Shaw cells, the symmetric arc-shaped ferrofluid pool is still formed around the magnet.

#### **4.5 Flow in Horizontal 2D Porous Media**

In the following experiments, ferrofluid was mobilized through sand beds by the magnetic attraction of a permanent magnet. The porous media consisted of shallow beds (1 cm thick) of the saturated S1 sand ( $K$ , hydraulic conductivity, =  $4.2 \times 10^{-2}$  cm/s,  $\phi = 0.46$ ) in trays with dimensions of 0.1 m x 0.12 m. After saturating the sand-filled trays with water, the sand surface

was smoothed and was left exposed. Ferrofluid was injected into the sand to form an initial ferrofluid distribution that was either approximately circular or was band-shaped across the width of the tray. An external field was then applied using the 5 stacked PM1 magnets. The ferrofluid movement through the sand was recorded using a video camera which was activated and time-indexed at appropriate intervals.

Typical results of a sand-bed experiment with an initial circular ferrofluid distribution are shown in Figure 10. In image (a), 0.5 ml of FF2 ferrofluid was injected into the sand tray at a distance of 0.1 m from one side of the tray. The magnet was then placed at the edge of the tray (the right side in the image) so that the center of the sand was on the  $y$ - $z$  plane of the magnetic pole at  $x = 0$  (see Figure 2). Images (b) and (c) depict the ferrofluid distribution at 23 and 43 minutes after injection. The flow of fluid toward the magnet is very similar to that observed in the Hele-Shaw cell experiments. The ferrofluid initially follows a direct pathway toward the center of the magnet. As the ferrofluid reaches the end of the tray, the magnet causes the ferrofluid to pool in a semi-circle.

The movement of ferrofluid from an initial band-shaped distribution is shown in Figure 11. 1.0 ml of FF1 was injected into the water-saturated S1 tray at 0.1 m from the edge of the plate. The images, a, b, c, and d in Figure 11 are at times 0, 2.77, 2.87, and 21 hours, respectively. In Figure 11b, several fingers of fluid (probably corresponding to the highest permeability pathways) break from the band and move toward the magnet. Figure 11c shows the fingers traveling to the magnet. As in the Hele-Shaw cell, the fluid accelerated as it approached the magnet, due to the higher magnetic field and steeper field gradient. Once a continuous path to

the magnet is established, accumulation of the fluid begins and the final ferrofluid distribution is very similar to that in the experiment with the circular initial ferrofluid distribution. The difference in the size of the final ferrofluid pool in the two experiments reflects the larger amount of ferrofluid in the band.

Experiments with larger S1 sand trays duplicated the same pattern of movement from distances of 0.25 m when the 5 stacked PM1 magnets were used. An image from the experiment at a time of 1 week is shown in Figure 12. As the distance from the magnet increased, the initial ferrofluid velocity decreased. As in the Hele-Shaw experiments, the process of deformation of the initial disk to a tear drop shape takes the majority of the time. As previously observed, as the fluid approaches the magnet, the velocity increases due to the increasing magnetic field strength and field gradient. This experiment illustrates dramatically that even if the forces are small due to a large magnet-ferrofluid separation, ferrofluid flow will still occur given sufficient time.

#### **4.6 Flow in Vertical 2-D Porous Medium**

An experiment in a vertical cell filled with water saturated S2 sand was conducted to observe the interaction of the magnetic field and gravity in the flow of a ferrofluid in porous media. The ferrofluid was injected 20 cm from the magnet as shown in Figure 13. As in the vertical Hele-Shaw experiment, the ferrofluid experiences both gravitational and magnetic forces as it migrates downward. In this case, magnetic forces dominate and the end point accumulation

is the familiar semi-circular pool, with a slight but discernible asymmetry due to the presence of gravity.

## 5. Discussion

The aim of the experiments presented here was to investigate the potential for controlling the emplacement of liquid in the subsurface through control of the external magnetic field. The experiments demonstrated that magnetic forces cause ferrofluid to flow over distances of order 0.25 m on timescales of hours to days. The forces generated can be quite large, rivaling those of gravity for density differences of the order of  $200 \text{ kg/m}^3$ . Furthermore, after being mobilized by magnetic forces, ferrofluids are held at steady state in a static and predictable arc-shaped configuration around the magnet.

These experimental observations have important implications for using ferrofluids for emplacement of viscous liquid barriers, treatment chemicals, and imagable tracers in the subsurface. For example, one possible application involves placing columns of magnets in boreholes around an isolation or treatment zone. Subsequent injection of ferrofluids with appropriate carrier liquids (barrier or reactants) would result in migration and accumulation against of liquid around the permanent magnets, creating a predictable and reproducible final structure. This process may be repeated to ensure complete coverage of a treatment area, or to produce overlapping barrier layers. Such barriers could be used for landfills or to seal leaking tanks or pipes. Another use would be to emplace ferrofluid, which by virtue of its high electrical conductivity and magnetic permeability, exerts a strong geophysical signal, for use as an imagable

tracer. Imagable tracers could be used to image the fracture zone, or for barrier verification where leaks would be detectable through geophysical surveys that locate ferrofluid.

Several important issues arise when considering the applicability of ferrofluids for subsurface fluid emplacement: (1) length scales; (2) dilution; (3) interaction with porous media and (4) stabilization with novel carrier liquids.

The most important issue concerns the length scales over which magnetic forces can be generated. The fact is that magnetic field strength ( $H$ ) declines rapidly with distance from the magnet. Since the force is proportional to the gradient of the magnetic field strength as well as the magnetization ( $M$ ) which is a strong function of  $H$  at low  $H$ , there is an even more rapid decline in force with distance from the magnet. Nevertheless, the experiments presented here demonstrate that ferrofluid can be mobilized by permanent magnets over length scales of order 0.25 m. And very near the magnet, magnetic forces can be quite large as observed in Figure 12 where the arc-shaped pool around the magnet is hardly affected by gravity even through the density difference is of order  $200 \text{ kg/m}^3$ . In general, we expect mobilization of ferrofluid over length scales greater than 1 m will be impractical, although superconducting electromagnets offer some hope of using stronger magnets to increase this length scale. Nevertheless, the strong attraction of ferrofluid to magnets over shorter length scales may be useful in subsurface applications, as discussed above, and can find immediate use in laboratory experiments where it is necessary to manipulate fluid in an apparatus without physically contacting the liquid.

The second issue we discuss is that of dilution. Specifically, ferrofluid will mix with groundwater in the subsurface by advection, dispersion, and molecular diffusion. Adsorption or

magnetic attraction of ferrofluid onto solid grains may dilute it further in groundwater. These processes will be augmented by the observed tendency of ferrofluid to be pulled in differing directions by gravitational and magnetic forces as it is attracted toward a permanent magnet. This tendency arises from the fact that ferrofluid closer to the magnet experiences significantly larger forces per unit volume than ferrofluid farther away. Thus an initially circular pool such as that in Figure 10 will be deformed and elongated. At the extreme are situations such as that in Figure 9 where part of the ferrofluid is pulled toward the magnet and part is pulled downward by gravity. Once ferrofluid is diluted, the strength of the magnetic body force on the mixture decreases and the ability to control emplacement is impaired. While some of these effects have been investigated [Borglin *et al.*, 1998], clearly more work is necessary to evaluate the importance of dilution in field applications.

The third issue is the interaction of ferrofluid with the porous media. Significant potential effects include filtration and reactions that could destabilize the ferrofluid. Our experiments to date show that sand has no adverse effects either through filtration or reaction, but we have yet to test fully a wide range of soil types. Any processes that can influence the magnetite-surfactant bond, including the effect of variations in the pore water chemistry, the change in ferrofluid particle size with dilution, bacterial action, and the strength of the magnetic field could irreversibly change the ferrofluid. This change could cause flocculation and sedimentation of the ferrofluid. This area should be the next area of experimental study.

The fourth issue is that of stabilization of the ferrofluid with carrier liquids such as viscous liquid barriers and other subsurface reactants. To date, ferrofluids have been stabilized



with a variety of mineral oils, water, and organic solvents [Berkovsky, 1996]. Other carrier liquids to be considered will have to be evaluated on a per case basis and will require further study.

## **6. Conclusions**

The experiments described here are aimed at investigating the potential for controlling the emplacement of ferrofluid in porous media. The multitude of observations in this study can be summarized by two main conclusions:

- (1) Permanent magnets create a predictable pressure gradient in a magnetic fluid that leads to fluid flow;
- (2) Ferrofluid can be driven through porous media to consistent and predictable final configurations, which are controlled solely by the magnetic field and are unaffected by the flow pathway or initial injection shape;

We emphasize that although our focus is ultimately on subsurface applications, ferrofluids may have immediate utility in laboratory work where the ability to manipulate fluids without pumping or contacting them directly is desirable. In general, our experiments offer a promising start to further investigations of ferrofluid applications for subsurface environmental applications. The development of this technology would provide a valuable tool for controlling liquid emplacement in the subsurface. This would be especially useful in situations where precise placement is paramount, or if excavation or pump and treatment methods are not possible due to high toxicity of the contaminants.

## 7. Acknowledgments

This work was supported by the Laboratory Directed Research and Development Program of Lawrence Berkeley National Laboratory under the U.S. Department of Energy, contract No. DE-AC03-76SF00098. The authors acknowledge helpful discussions with Alex Becker, Ross Schlueter, and Dr. K. Raj during the course of this work. We thank John Apps and Peter Persoff for their careful review of this report.

## 8. References

Berkovsky, B.M.: *Magnetic Fluids and Applications Handbook*, Begell House, Inc., New York, 1996.

Borglin, S.E., G.J. Moridis, and C.M. Oldenburg, *Experimental Studies of Magnetically-Driven Flow of Ferrofluids in Porous Media*. Lawrence Berkeley National Laboratory Report LBL-40126, Berkeley, California, August, 1998.

Chorney, A.F., and W. Mraz, W, Hermetic sealing with magnetic fluids, *Machine Design*, 9, 79-82, 1992.

Lamb, H: *Hydrodynamics*, Dover, New York, 1945.

McCaig, M. and A.G. Clegg, *Permanent magnets in theory and practice*. 2nd ed., John Wiley and Sons, New York, 1987.

- Moridis, G.J., S.E. Borglin, C.M. Oldenburg, and A. Becker, *Theoretical and experimental investigations of ferrofluids for guiding and detecting liquids in the subsurface*. Lawrence Berkeley National Laboratory Report LBL-41069, Berkeley, California, March, 1998.
- Moridis, G.J., and C.M. Oldenburg, *Ferrofluid Flow in Porous Media*, Lawrence Berkeley National Laboratory Report LBL-41486, Berkeley, California, March, 1998.
- Nunes, A.C. and Z.C. Yu, Fractionation of a water-based Ferrofluid, *J. of Magnetism and Magnetic Materials*, 65, 265-268, 1987.
- Oldenburg, C.M., S.E. Borglin, and G.J. Moridis, *Numerical simulation of ferrofluid flow for subsurface environmental engineering applications*. submitted to *Transport in Porous Media*, also Lawrence Berkeley National Laboratory Report LBL-40146, Berkeley, California, June, 1998.
- Raj, K and R. Moskowitz, Commercial applications of ferrofluid, *J. of Magnetism and Magnetic Materials*, 85, 233-245, 1990.
- Rosensweig, R.E.: *Ferrohydrodynamics*. Cambridge University Press, Cambridge, 1985.
- Saffman, P.G., and G.I. Taylor, The penetration of a fluid into a porous medium or Hele-Shaw cell containing a more viscous liquid, *Proc. Roy Soc. London Ser. A*, 245, 312-29, 1958.
- Schroth, M.H., S.J. Ahearn, J.S. Selker, and J.D. Istok. Characterization of Miller-Similar Silica Sands for Laboratory Hydrologic Studies. *J. Soil Sci. Soc. Am.*, 60 1331-1339, 1996.

## 9. List of Tables and Figures

**Table 1.** Physical Properties of EMG 805<sup>TM</sup> (FF1) and EMG-C<sup>TM</sup> (FF2) ferrofluid (Ferrofluidics Corporation, Nashua, NH).

**Table 2.** Physical Properties of Monterey #60 sand, and Unimin 30/40 mesh silica sand.

**Table 3.** Properties of the NdFeB Magnets.

**Figure 1.** Magnetization Curve for EMG 805<sup>TM</sup> (FF1 ferrofluid)

**Figure 2.** Permanent Magnet Configuration

**Figure 3.** Predicted and measured magnetic field from 5 stacked PM1 magnets. Dimensions of the magnet and parameters of magnet strength are given in Table 3.

**Figure 4.** Schematic of magnetopressure measurement apparatus **Figure 5.** Measured and predicted pressures for FF2 (EMG-C<sup>TM</sup>) ferrofluid using the five stacked PM1 magnets and the PM2 magnet.

**Figure 6.** Measured and predicted pressures for FF2 (EMG-C<sup>TM</sup>) and FF1 (EMG 805<sup>TM</sup>) ferrofluids using the five stacked PM1 magnets.

**Figure 7.** Top and side views of a typical horizontal Hele-Shaw cell used to observe ferrofluid movement. The position of the magnet and the injection point shown in the top view varies according to experiment.

**Figure 8.** Progression of FF1 ferrofluid through water-filled horizontal Hele-Shaw cell. The magnetic field was produced by five stacked PM1 magnets. Frames a, b, c, and d are at times 0, 219, 277, and 427 seconds, respectively.

**Figure 9.** Movement of FF1 ferrofluid through a vertical Hele-Shaw cell. Five stacked PM1 magnets are located at the left side of the frame. Three injection points are shown in the figure: (1) 17 cm from magnet, showing 100 % travel to magnet, (2) 20 cm from the magnet showing partial travel to magnet, partial fall under gravity, and (3) 22 cm showing 100 % fall to bottom.

**Figure 10.** Movement of FF2 ferrofluid with an initial circular injection through water-saturated S1 sand. Frames are at 0, 23, and 43 minutes.

**Figure 11.** Movement of FF2 ferrofluid with an initial band-shaped injection through water-saturated S1 sand. Times are 0, 2.77, 2.87, and 21 hours.

**Figure 12.** FF2 ferrofluid movement through water-saturated S1 sand. Five stacked PM1 magnets are located on the center of the right side of the tray. Initial ferrofluid injection into the sand was circular at a distance of 0.25 m from the face of the magnet. The figure shows the system seven days after initial injection.

**Figure 13.** Movement of FF2 ferrofluid through a vertically oriented cell filled with S2 sand. Magnet is located in the center of the left side. Time elapsed is 75 minutes.



**Table 1.** Physical Properties of EMG 805<sup>TM</sup> (FF1) and EMG-C<sup>TM</sup> (FF2) ferrofluid (Ferrofluidics Corporation, Nashua, NH).

Property	EMG 805 <sup>TM</sup> (FF1)	EMG-C <sup>TM</sup> (FF2)
Viscosity, $\mu$ , at 27°C	0.0025 Pa·s	0.008 Pa·s
Magnetite Concentration	3.7 %	5.2 %
Surfactant Concentration	8 %	10 %
Water Concentration	88.3 %	84.8 %
Initial Magnetic Susceptibility	6.16 (MKS units)	6.16 (MKS units)
pH	7	7
Density	1190 kg/m <sup>3</sup>	2000 kg/m <sup>3</sup>
Saturation Magnetization	1.6 x 10 <sup>4</sup> A/m	3.1 x 10 <sup>4</sup> A/m

**Table 2.** Physical Properties of Monterey #60 sand, and Unimin 30/40 mesh silica sand.

Soil	Designation	Porosity, $\phi$	Hydraulic Conductivity, $K$ , (m/s)	D <sub>10</sub> (mm)
Monterey #60	S1	0.46	4.2 x 10 <sup>-5</sup>	0.23
Unimin 30/40 mesh	S3	0.33	1.5 x 10 <sup>-3</sup> [Schroth et al., 1996]	0.45 [Schroth et al., 1996]

**Table 3.** Properties of the NdFeB Magnets.

Magnet Type	Description	Field Strength	Dimensions
NdFeB (PM1)	Permanent magnet, Rectangular shape	$B_r = 1.2$ T $H_c = 1.0 \times 10^5$ A/m	$L_o = 0.0254$ m $2a = 0.05$ m $2b = 0.05$ m
NdFeB (PM2)	Permanent magnet, Rectangular shape	$B_r = 1.1$ T $H_c = 0.93 \times 10^5$ A/m	$L_o = 0.0254$ m $2a = 0.035$ m $2b = 0.035$ m



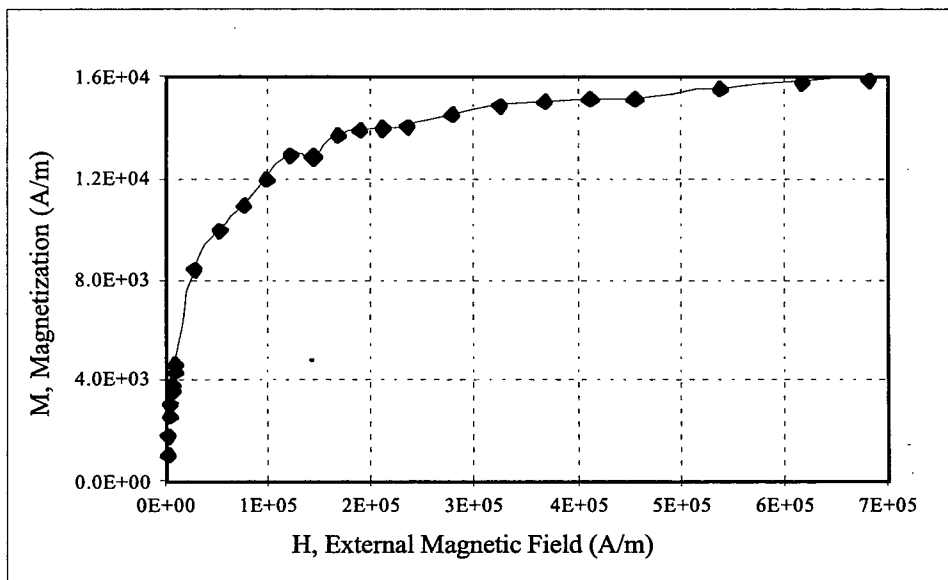


**Figure 1.** Magnetization Curve for EMG 805™ (FF1 ferrofluid)

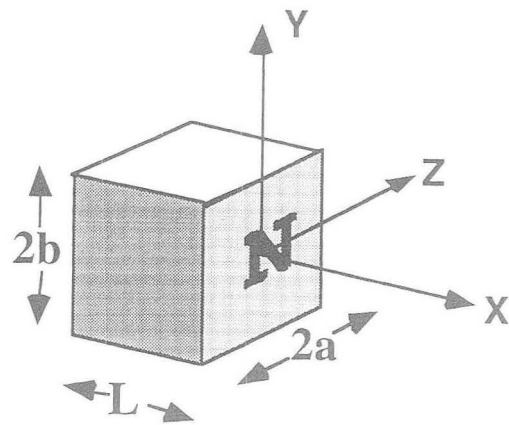
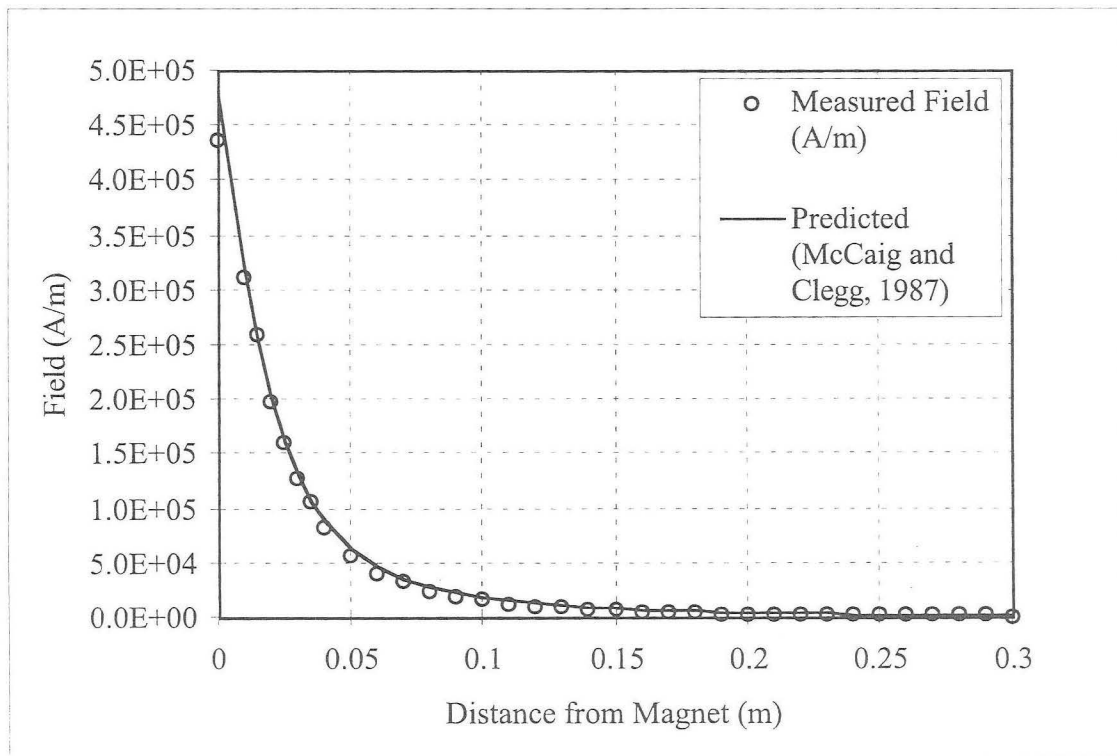


Figure 2. Permanent Magnet Configuration



**Figure 3.** Predicted and measured magnetic field from 5 stacked PM1 magnets. Dimensions of the magnet and parameters of magnet strength are given in Table 3.

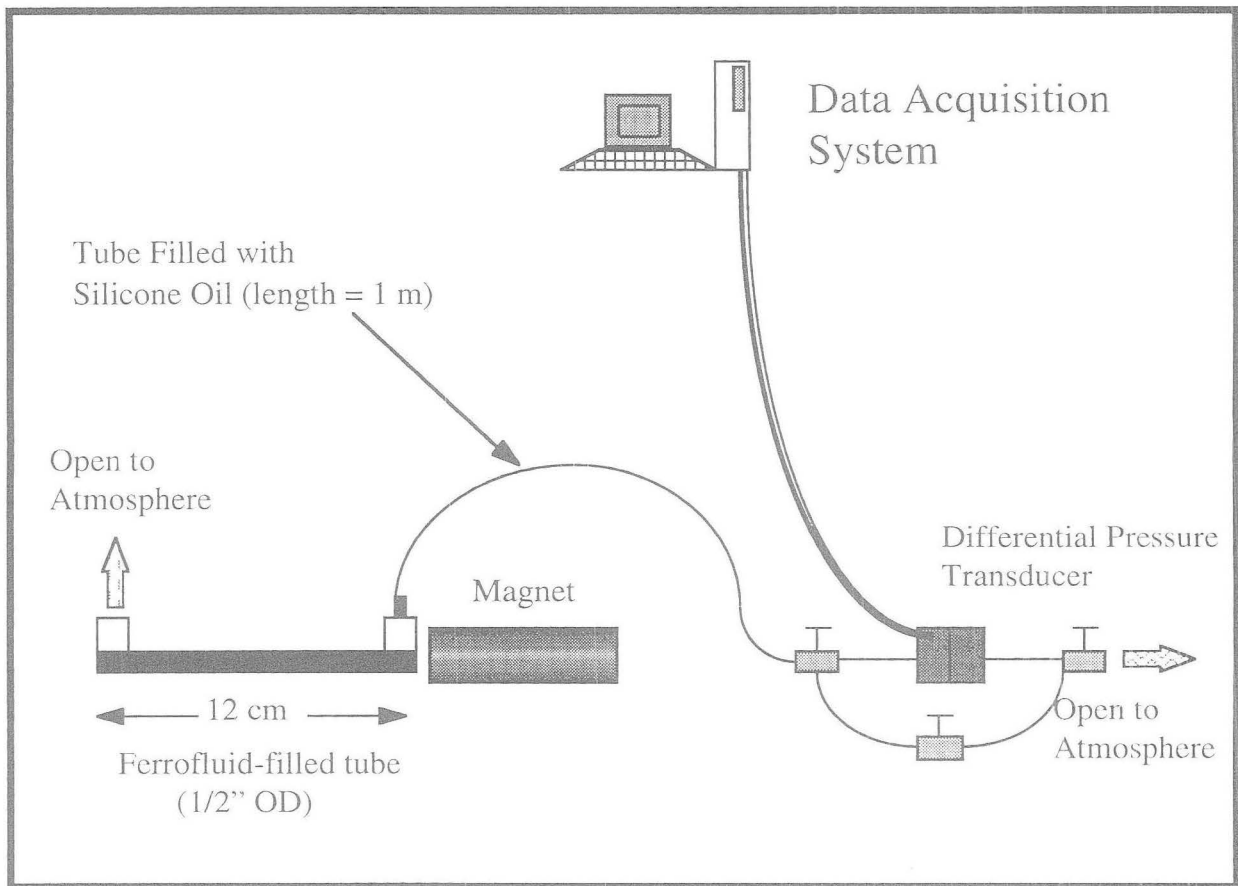
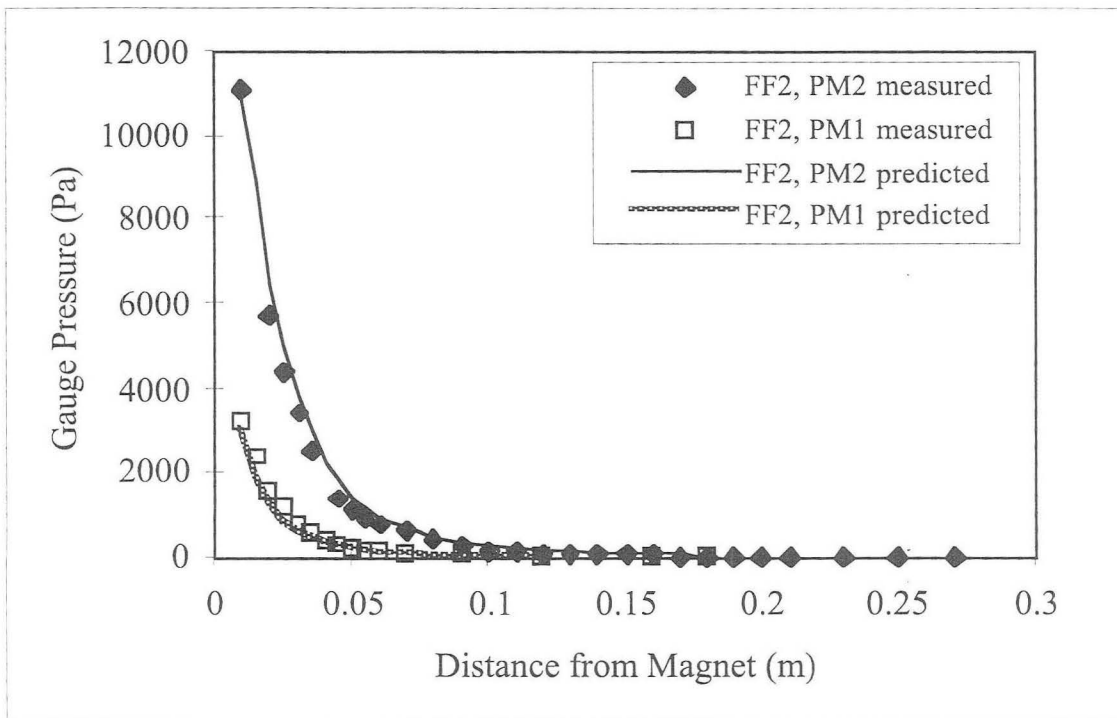


Figure 4. Schematic of magnetopressure measurement apparatus



**Figure 5.** Measured and predicted pressures for FF2 (EMG-C™) ferrofluid using the five stacked PM1 magnets and the PM2 magnet.

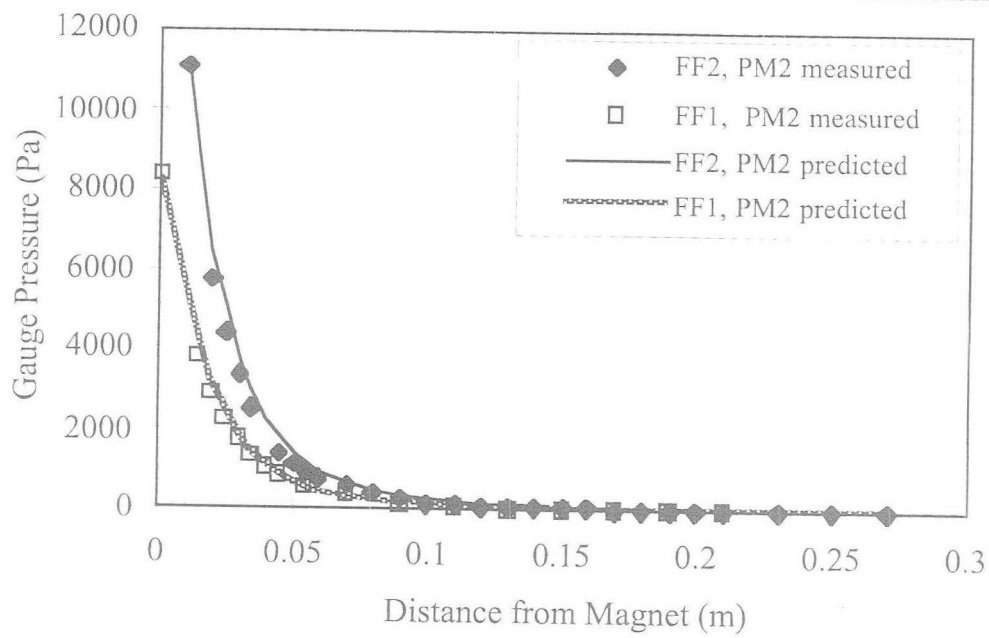
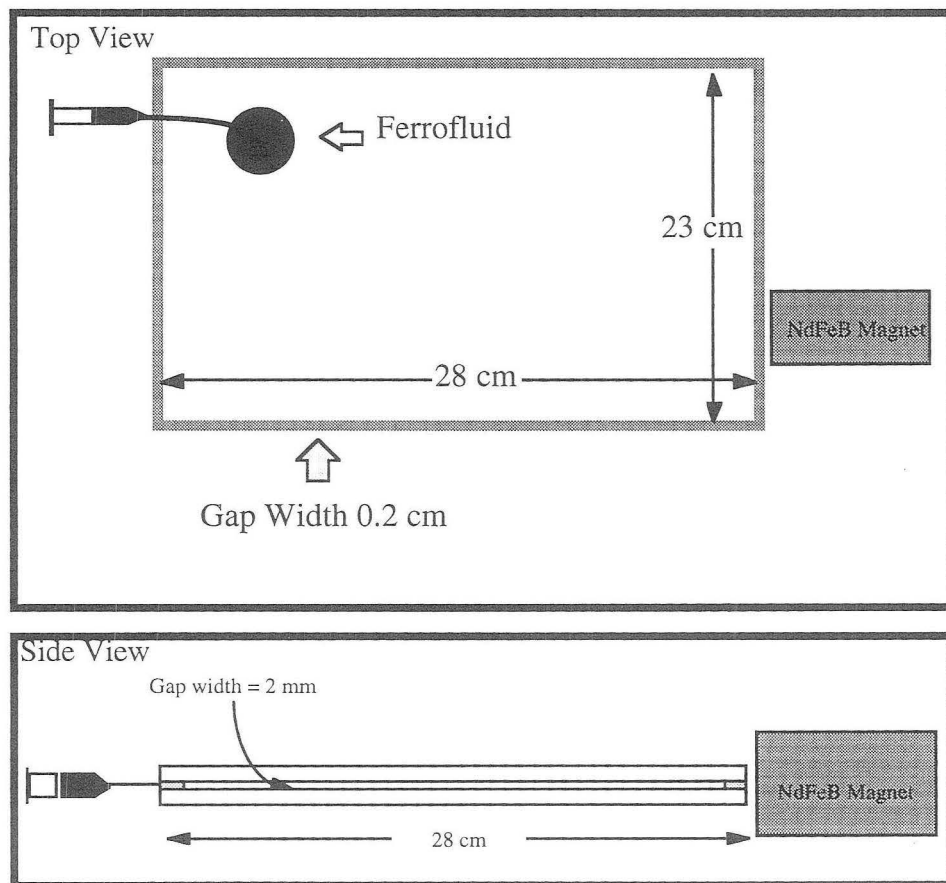
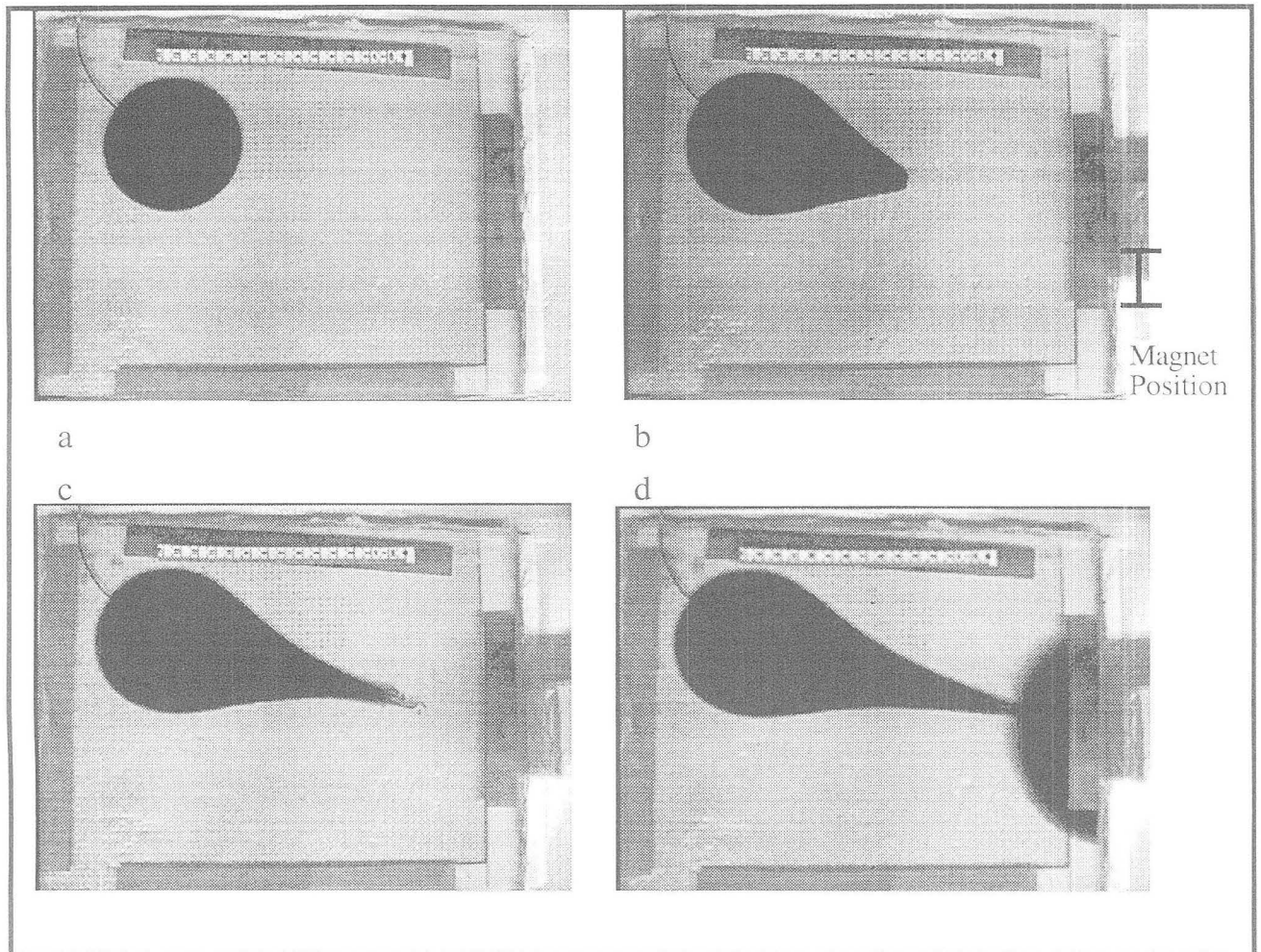


Figure 6. Measured and predicted pressures for FF2 (EMG-C™) and FF1 (EMG 805™) ferrofluids using the five stacked PM1 magnets.



**Figure 7.** Top and side views of a typical horizontal Hele-Shaw cell used to observe ferrofluid movement. The position of the magnet and the injection point shown in the top view varies according to experiment.



**Figure 8.** Progression of FF1 ferrofluid through water-filled horizontal Hele-Shaw cell. The magnetic field was produced by five stacked PM1 magnets. Frames a, b, c, and d are at times 0, 219, 277, and 427 seconds, respectively.



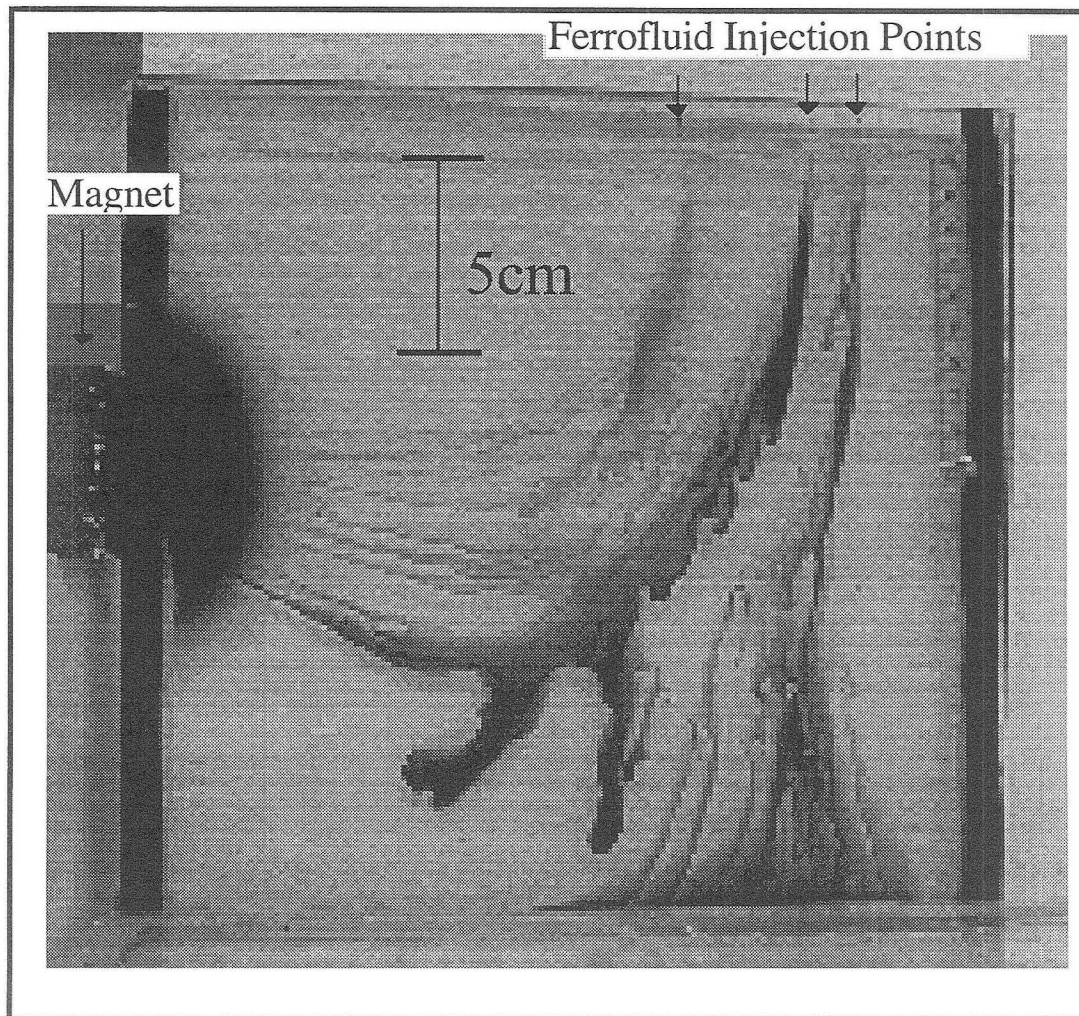


**Figure 9.** Movement of FF1 ferrofluid through a vertical Hele-Shaw cell. Five stacked PM1 magnets are located at the left side of the frame. Three injection points are shown in the figure: (1) 17 cm from magnet, showing 100 % travel to magnet, (2) 20 cm from the magnet showing partial travel to magnet, partial fall under gravity, and (3) 22 cm showing 100 % fall to bottom.

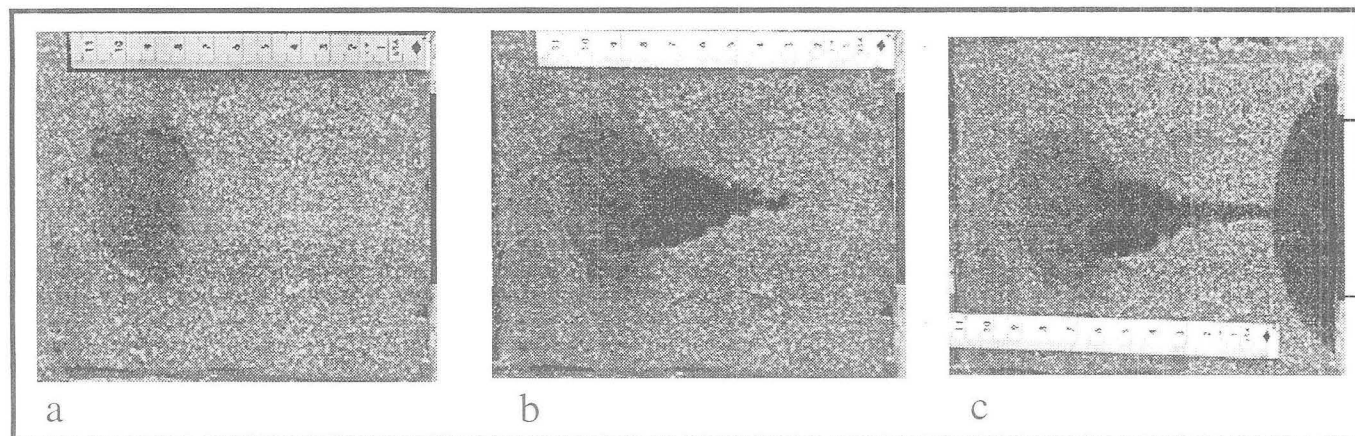


**Figure 10.** Movement of FF2 ferrofluid with an initial circular injection through water-saturated S1 sand. Frames are at 0, 23, and 43 minutes.

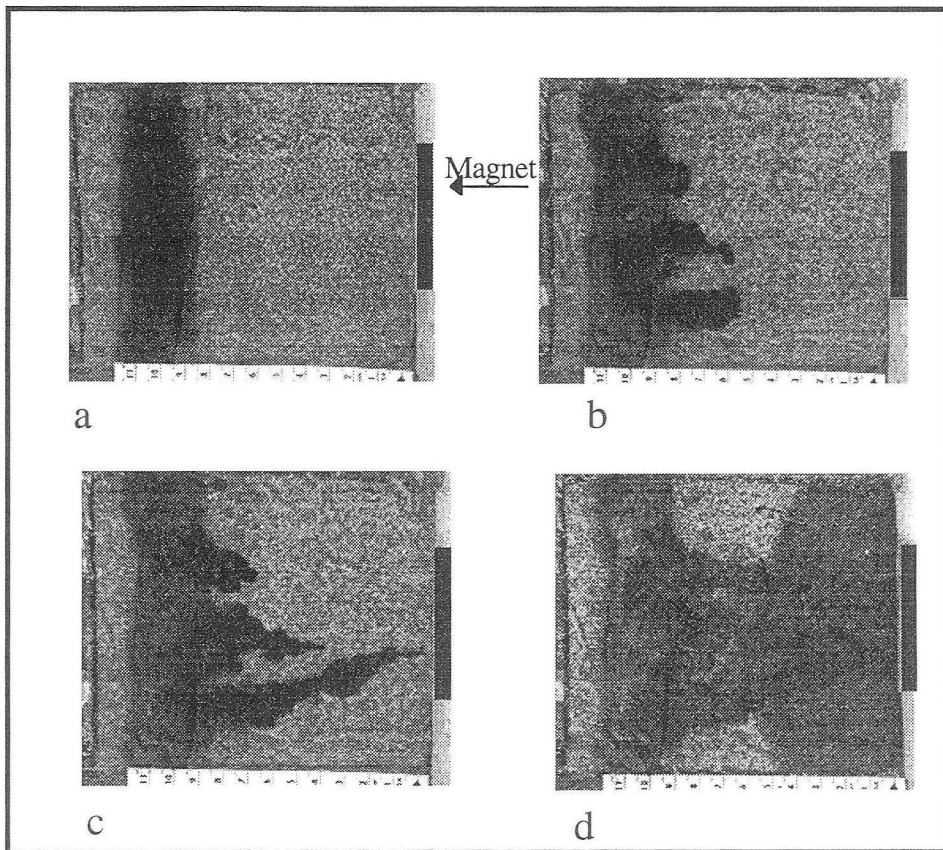


**Figure 11.** Movement of FF2 ferrofluid with an initial band-shaped injection through water-saturated S1 sand. Times are 0, 2.77, 2.87, and 21 hours.

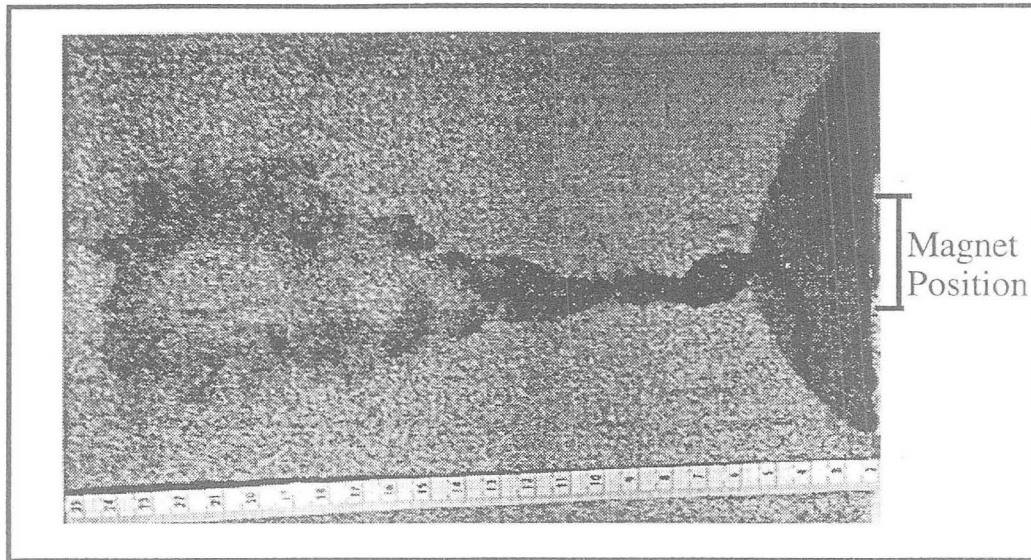


**Figure 12.** FF2 ferrofluid movement through water-saturated S1 sand. Five stacked PM1 magnets are located on the center of the right side of the tray. Initial ferrofluid injection into the sand was circular at a distance of 0.25 m from the face of the magnet. The figure shows the system seven days after initial injection.

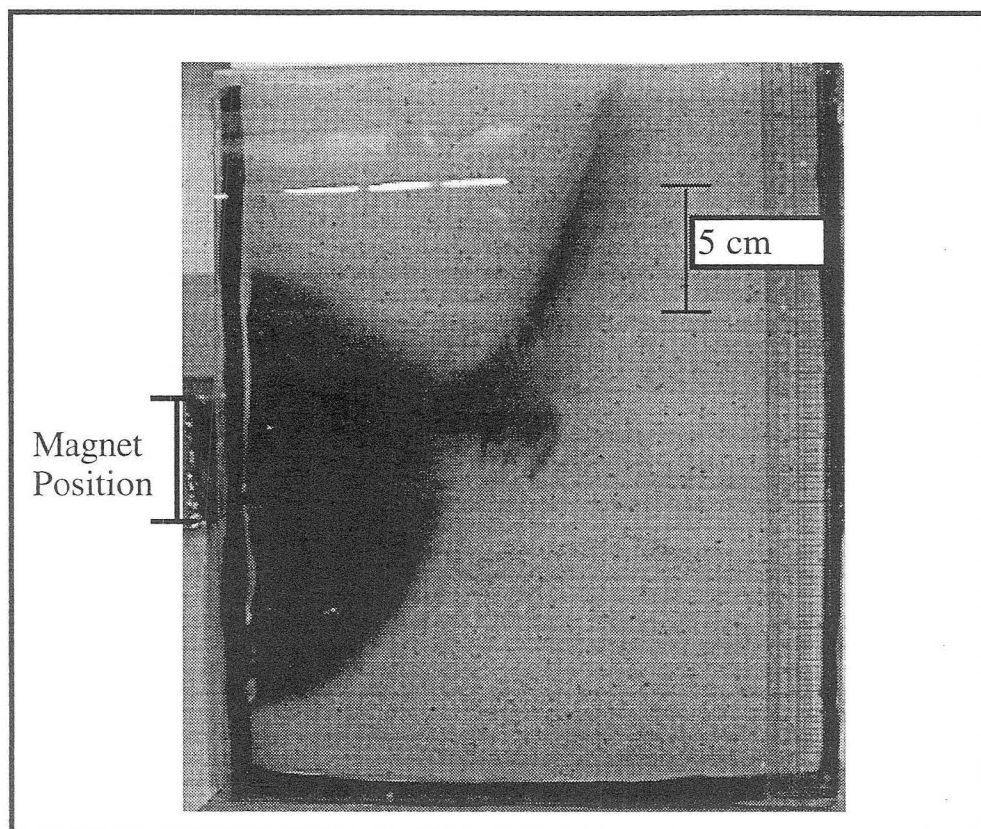


**Figure 13.** Movement of FF2 ferrofluid through a vertically oriented cell filled with S2 sand. Magnet is located in the center of the left side. Time elapsed is approximately 75 minutes.

**ERNEST ORLANDO LAWRENCE BERKELEY NATIONAL LABORATORY**  
**ONE CYCLOTRON ROAD | BERKELEY, CALIFORNIA 94720**